Effective Scattering Control of Graphene Micro-disks Utilizing the Fundamental Plasmon Resonances

Stamatios Amanatiadis[1*], Vasileios Salonikios[1], Michalis Nitas[1], Theodoros Zygiridis[2], Nikolaos Kantartzis[1], and Traianos Yioultsis[1]

[1]Department of Electrical and Computer Engineering, Aristotle University of Thessaloniki, Thessaloniki, Greece
[2]Department of Electrical and Computer Engineering, University of Western Macedonia, Kozani, Greece
*corresponding author, E-mail: samanati@auth.gr

Abstract

The plane wave scattering on graphene micro-disks is investigated numerically in the present work. Initially, the propagation properties of the supported surface waves on the 2D material are studied theoretically. Then, the plasmonic resonant frequencies of a circular graphene scatterer are identified via the broadband analysis of the absorption cross-section. Finally, the radar cross-section of the same setup is examined, indicating that the resonant frequencies are optimal for forward propagation, thus enabling the effective beam manipulation.

1. Introduction

Several years have passed since the first report of a stable graphene layer, but various different aspects regarding this truly 2D material are still challenging. Specifically, the capability of graphene to support surface waves at the far-infrared regime has enabled the design of various devices [1]. However, the theoretical analysis is limited on infinite layers, while numerical solvers are required for the characterization of plasmonic waveguides [2, 3].

This paper focuses on a circular graphene scatterer to identify its resonant frequencies. This is achieved through the absorption cross-section numerical examination of a plane-wave that propagates towards our device. Moreover, the radar cross-section is investigated at various frequencies, indicating that forward propagation is maximized at resonances. This knowledge is important since an effective beam manipulation is enabled via the appropriate combination of graphene scatterers on 2D arrays [4].

2. Theoretical aspects and setup

2.1. Graphene surface conductivity

In our work, graphene is considered as a thin layer, characterized via its surface conductivity $\sigma_{\rm gr}$. The latter depend on the chemical potential μ_c, the scattering rate Γ , and the temperature T and it is evaluated by the compact expression resulting from the Kubo formula [5], involving only the dominant, at the far-infrared spectrum, intraband term:

$$\sigma_{\rm gr} = \frac{e^2 k_B T}{\pi\hbar^2(j\omega + 2\Gamma)}\left[\frac{\mu_c}{k_B T} + 2\ln(e^{-\frac{\mu_c}{k_B T}} + 1)\right]. \quad (1)$$

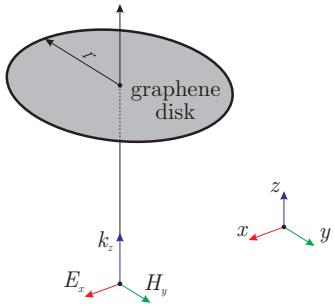

Figure 1: Linearly polarized plane-wave propagating towards a graphene circular scatterer.

2.2. Surface wave propagation properties

The propagation properties of the surface wave onto graphene are evaluated via the complex wavenumber k_ρ that is extracted via [6]:

$$k_\rho = k_0\sqrt{1 - \left(\frac{2}{\sigma_{\rm gr}\eta_0}\right)^2}, \quad (2)$$

with k_0 and η_0 the free space wavenumber and wave impedance, respectively. An additional, more intuitive feature of the SPP wave is its wavelength λ_{SPP} that is related to k_ρ via $\lambda_{SPP} = 2\pi/\Re\{k_\rho\}$.

2.3. Setup description

The main device of this work is a circular graphene scatterer of radius r, as depicted in Fig. 1. The selection of such a simple apparatus initiates from its symmetrical configuration. Therefore, the scattering effects are independent of the plane wave polarization that is propagating perpendicularly to the surface.

3. Numerical Analysis

3.1. Computational setup

Our setup is investigated using the popular FDTD method, and the computational domain is divided into $100 \times 100 \times 400$ cells with $\Delta x = \Delta y = \Delta z = 2\,\mu$m. Moreover, a time-step of $\Delta t = 3.8$ fs is selected and open boundaries are terminated with an 8-cell perfectly matched layer. The sim-

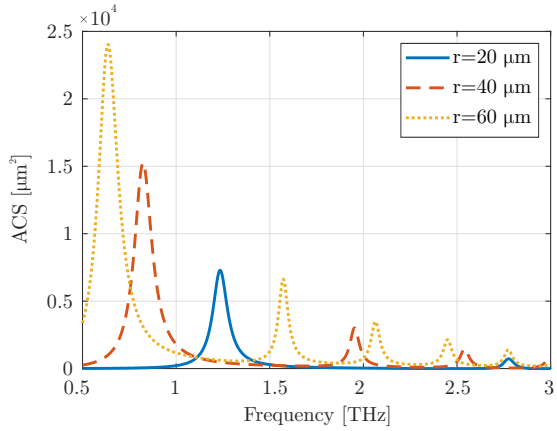

Figure 2: Absorption cross-section of graphene circular scatterers with different radii.

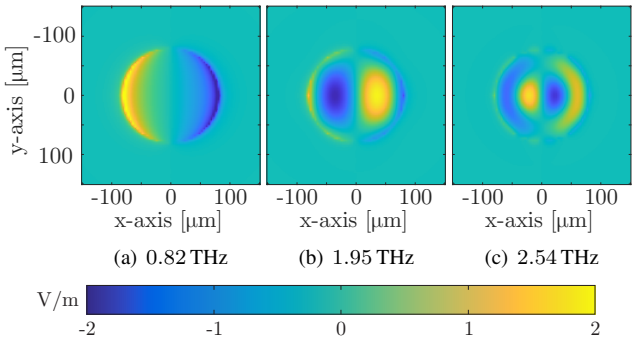

Figure 3: Distribution of the normal, to graphene disk, electric component at different resonance frequencies.

ulations are conducted within the range $0.5 - 3$ THz, where graphene plasmonic waves are strong, while the radius of the circular scatterer varies from $r = 20\,\mu$m to $60\,\mu$m. Finally, graphene parameters are set to $\Gamma = 0.1$ meV and the chemical potential varies from low to moderate values, specifically $0.1 - 0.3$ eV.

3.2. Numerical results

Initially, the broadband absorption cross-section (ACS) is extracted for the graphene disks. This operation facilitates the identification of the resonant frequencies since the ACS peaks highlight the regions of increased absorption. The numerical results for the involved graphene disks are depicted in Fig. 2 and it is evident that various resonances are present. Moreover, their number increases with the radius.

Interestingly, the first mode appears at the frequency that $\lambda_{\rm SPP}$ is equal to the disk's circumference. Additionally, the subsequent modes are at $r = n\lambda_{\rm SPP}/4$ with $n = 3, 5, 7, \ldots$. The electric field distribution at the resonant frequencies, in Fig. 3, indicates that the first mode is concentrated along the edge of the disk, while the higher-order ones are stronger at its interior.

Finally, the radar cross-section is sketched in Fig. 4 for the graphene disk with $r = 40\,\mu$m. Although the back-scattered wave is independent of the frequency, the for-

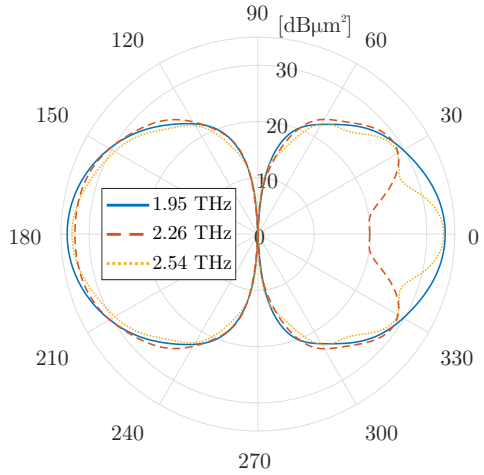

Figure 4: Radar cross-section of a graphene circular scatterer ($r = 40\,\mu$m) at different frequencies.

ward scattering differentiates. Specifically, at the resonant frequencies, 1.95 THz and 2.54 THz, the initial direction is preserved, in contrast to the non-resonant ones that the plane-wave is scattered sideways.

Acknowledgement

The research project was supported by the Hellenic Foundation for Research and Innovation (H.F.R.I.) under the "2nd Call for H.F.R.I. Research Projects to support Post-Doctoral Researchers" (Project Number: 756).

References

[1] J. Garcia de Abajo, Graphene plasmonics: challenges and opportunities, *ACS Photonics* 1(3): 135–152, 2014.

[2] V. Salonikios *et al.*, Modal analysis of graphene microtubes utilizing a two-dimensional vectorial finite element method, *Appl. Phys. A* 122(4): 1–7, 2016.

[3] V. Salonikios *et al.*, Computational analysis of graphene-based periodic structures via a three-dimensional field-flux eigenmode finite element formulation, *Prog. Electromagn. Res. M* 92: 157–167, 2020.

[4] O. Tsilipakos *et al.*, Toward intelligent metasurfaces: the progress from globally tunable metasurfaces to software-defined metasurfaces with an embedded network of controllers, *Adv. Opt. Mater.* 8(17): 2000783, 2020.

[5] V. P. Gusynin, S. G. Sharapov, and J. P. Carbotte, Magneto-optical conductivity in graphene, *J. Phys. Condens. Matter* 19(2): 026222, 2006.

[6] G. W. Hanson, Dyadic Green's functions and guided surface waves for a surface conductivity model of graphene, *J. Appl. Phys.* 103(6): 064302, 2008.